JIM Original Article

doi: 10.1111/joim.13674

Parallel testing of liquid biopsy (ctDNA) and tissue biopsy samples reveals a higher frequency of *EZH2* mutations in follicular lymphoma

Ákos Nagy[1], Bence Bátai[1], Laura Kiss[1], Stefánia Gróf[1], Péter Attila Király[2], Ádám Jóna[3], Judit Demeter[4], Hermina Sánta[5], Árpád Bátai[5], Piroska Pettendi[6], Tamás Szendrei[7], Márk Plander[7], Gábor Körösmezey[8], Hussain Alizadeh[9], Béla Kajtár[10], Gábor Méhes[11], László Krenács[12], Botond Timár[1], Judit Csomor[1], Erika Tóth[13], Tamás Schneider[2], Gábor Mikala[14], András Matolcsy[1,15], Donát Alpár[1], András Masszi[2] & Csaba Bödör[1]

From the [1]HCEMM-SE Molecular Oncohematology Research Group, Department of Pathology and Experimental Cancer Research, Semmelweis University, Budapest, Hungary; [2]Hematology and Lymphoma Unit, National Institute of Oncology, Budapest, Hungary; [3]Department of Hematology, Faculty of Medicine, Medical School of Clinical Medicine, University of Debrecen, Debrecen, Hungary; [4]Department of Internal Medicine and Oncology, Semmelweis University, Budapest, Hungary; [5]Szent György Hospital of County Fejér, Székesfehérvár, Hungary; [6]Hetényi Géza Hospital, Clinic of County Jász-Nagykun-Szolnok, Szolnok, Hungary; [7]Markusovszky University Teaching Hospital, Szombathely, Hungary; [8]Department of Medicine, Military Hospital - Medical Centre, Hungarian Defence Forces, Budapest, Hungary; [9]1st Department of Internal Medicine, Medical School, University of Pécs, Pécs, Hungary; [10]Department of Pathology, Medical School, Clinical Centre, University of Pécs, Pécs, Hungary; [11]Department of Pathology, Faculty of Medicine, University of Debrecen, Debrecen, Hungary; [12]Laboratory of Tumor Pathology and Molecular Diagnostics, Szeged, Hungary; [13]Department of Surgical and Molecular Pathology, National Institute of Oncology, Budapest, Hungary; [14]Department of Hematology and Stem Cell Transplantation, National Institute for Hematology and Infectious Diseases, South Pest Central Hospital, Budapest, Hungary; and [15]Department of Laboratory Medicine, Karolinska Institutet, Solna, Sweden

Abstract. Nagy Á, Bátai B, Kiss L, Gróf S, Király PA, Jóna Á, et al. Parallel testing of liquid biopsy (ctDNA) and tissue biopsy samples reveals a higher frequency of *EZH2* mutations in follicular lymphoma. *J Intern Med.* 2023;**00**:1–19.

Background. Recent genomic studies revealed enhancer of zeste homolog 2 (*EZH2*) gain-of-function mutations, representing novel therapeutic targets in follicular lymphoma (FL) in around one quarter of patients. However, these analyses relied on single-site tissue biopsies and did not investigate the spatial heterogeneity and temporal dynamics of these alterations.

Objectives. We aimed to perform a systematic analysis of *EZH2* mutations using paired tissue (tumor biopsies [TB]) and liquid biopsies (LB) collected prior to treatment within the framework of a nationwide multicentric study.

Methods. Pretreatment LB and TB samples were collected from 123 patients. Among these, 114 had paired TB and LB, with 39 patients characterized with paired diagnostic and relapse samples available. The *EZH2* mutation status and allele burden were assessed using an in-house-designed, highly sensitive multiplex droplet digital PCR assay.

Results. *EZH2* mutation frequency was found to be 41.5% in the entire cohort. In patients with paired TB and LB samples, *EZH2* mutations were identified in 37.8% of the patients with mutations exclusively found in 5.3% and 7.9% of TB and LB samples, respectively. *EZH2* mutation status switch was documented in 35.9% of the patients with paired diagnostic and relapse samples. We also found that *EZH2* wild-type clones may infiltrate the bone marrow more frequently compared to the *EZH2* mutant ones.

Conclusion. The in-depth spatio-temporal analysis identified *EZH2* mutations in a considerably higher proportion of patients than previously reported. This expands the subset of FL patients who most likely would benefit from EZH2 inhibitor therapy.

Keywords: ctDNA, ddPCR, *EZH2*, follicular lymphoma, liquid biopsy, tazemetostat

Introduction

Follicular lymphoma (FL) is the most common indolent non-Hodgkin lymphoma (NHL) characterized by a long median overall survival of approximately 15–20 years [1, 2]. Despite its indolent nature, the disease remains incurable and is associated with multiple relapses in the majority of patients. In approximately 10% of the cases, high-grade transformation to a more aggressive lymphoma occurs within 5 years [3].

Significant advancements were made in the last decade in understanding the genetic background of FL [4–9]. Strikingly, nearly all FL patients carry molecular alterations in at least one of the epigenetic modifiers [10–12]. One of the most common alterations affecting the epigenetic machinery is the gain-of-function mutations of enhancer of zeste homolog 2 (*EZH2*), previously detected in up to 27% of all cases, in studies predominantly focusing on the analysis of single tissue biopsies [4, 13–17]. The seven different activating mutations of this gene affect the catalytic SET domain of the protein and are located in exon 16 (p.Y646F/N/H/C/S) and exon 18 (p.A682G and p.A692V). These alterations are considered early clonal events. However, cases with *EZH2* mutation restricted to disease progression or relapse were also described [7, 14, 15]. Tazemetostat—a first-in-its-class small molecular inhibitor of EZH2—has recently been approved in the United States for the treatment of relapsed/refractory FL with *EZH2* mutations [18–21], making *EZH2* the first target in FL for precision oncology. Tazemetostat showed superior activity in patients harboring *EZH2* mutations [19]. Consequently, diagnostic tests able to detect these alterations reliably and sensitively are needed.

Although histological analysis of tumor biopsies (TB) remains the cornerstone in the diagnosis of NHLs, it is well established that a single TB does not necessarily represent a spatially heterogeneous disease such as FL [22, 23]. Detection and analysis of circulating cell-free DNA (cfDNA)—also known as liquid biopsy (LB)—can overcome this limitation and recover genetic alterations restricted to sites not captured by tissue biopsy [24, 25]. Circulating tumor DNA (ctDNA) fraction of cfDNA usually has a low abundance in indolent diseases such as FL [26]. Therefore, sensitive techniques—including next-generation sequencing (NGS) or droplet digital PCR (ddPCR)—are required [27–29]. Moreover, the amount of ctDNA may more precisely represent the total tumor burden compared to currently used imaging-based methods and may convey valuable ancillary information for staging in the future. Indeed, the prognostic role of ctDNA is being increasingly recognized. However, limited data is available on the potential clinical relevance of liquid biopsy in FL.

The minimal invasivity of liquid biopsy allows for serial sampling, enabling longitudinal therapy monitoring. Treatment monitoring in FL is performed by imaging-based methods, mainly PET/CT—18F-fluorodeoxyglucose positron emission tomography combined with computer tomography—which is hampered by its limited sensitivity and specificity, leading to difficulties in interpreting cases with residual metabolic activity [30, 31]. On the contrary, liquid biopsy may offer a rapid, radiation-free, sensitive disease monitoring alternative with better resolution [32].

Alongside ctDNA, circulating tumor cells (CTC) can be detected and monitored in the blood peripheral mononuclear cell (PBMNC) fraction in the majority of patients with FL [33–35]. Although ctDNA appears to be more abundant in the peripheral blood prior to therapy compared to CTCs with data mainly restricted to high-grade lymphomas, it is still debated which method would be more applicable for minimally invasive detection and monitoring in the future for low-grade lymphomas, including FL [36].

In this study, we aimed to perform a systematic analysis of *EZH2* mutations using paired tissue and LB collected prior to treatment and during therapy within the framework of a nationwide multicentric study. We also tested whether pretreatment *EZH2* variant allele frequencies (VAF) mirror tumor burden and extent, compared to clinical, radiological, and histological parameters. To our knowledge, this is the first spatio-temporal analysis of *EZH2* mutations in paired tissue and LB using a highly sensitive, self-developed multiplex droplet digital PCR approach in a multicenter FL patient cohort.

András Masszi and Csaba Bödör are senior authors.

Patients and methods

Sample recruitment and patient information

Paired pretreatment LB and TB samples were obtained from 114 FL patients treated in 10 Hungarian hematology centers. Seventy-seven patients were recruited at the time of diagnosis, 36 at the time of relapse and 1 patient had paired TB and LB samples at both timepoints. Detailed histological, clinical, and radiological information of the patient cohort is provided in Table S1. Additionally, 69 LB samples were collected longitudinally at the first day of the treatment cycles from 19 patients (from the same cohort) being actively treated, with two–six sequential samples per patient. Samples collected during surveillance were also analyzed in 12 patients (from the same cohort). LB samples from nine progressing/relapsed patients who lacked paired relapse TB samples were also included. Altogether, we analyzed 181 LB, 215 TB, and 53 PBMNC samples collected from 123 FL patients. All patients had at least one TB with histologically confirmed FL (grade 1–3 A) with patients presenting exclusively with grade 3B or transformed histology excluded from the study. *EZH2* mutation status from PBMNC samples (potential CTCs) was investigated if the corresponding LB sample collected at the same time proved to be *EZH2* mutant.

Relapse was defined as progression after at least one previous line of therapy or at least 12 months of watch and wait approach without therapy. The study was conducted in accordance with the Declaration of Helsinki, and the protocol was approved by the Ethics Committee of the Hungarian Medical Research Council (45371-2/2016/EKU and IV/5495-3/2021/EKU).

DNA isolation from LB samples

LB samples were collected using Cell-Free DNA Collection Tubes (Roche, Switzerland). Plasma fraction of 3–4 mL volume was isolated using a two-step centrifugation protocol (whole blood was centrifuged at 1600*g* for 20 min at 4°C, subsequently the plasma fraction was centrifuged at 16,000*g* for 10 min at 4°C), then plasma samples were frozen at −20°C and stored at −70°C for a prolonged time until further processing. cfDNA was isolated using the QIAamp Circulating Nucleic Acid Kit (Qiagen, Germany) following the manufacturer's instructions. Isolated cell-free DNA samples were stored at −20°C. Quantity and quality of cfDNA were assessed by a Qubit 4 Fluorometer (Thermo Fisher Scientific, USA) and 4200 TapeStation System (Agilent Technologies, USA), respectively.

DNA isolation from TB samples

Lymph node, bone marrow (BM), or extranodal tissue samples were available from 125 patients for tumor DNA isolation from formalin-fixed paraffin embedded tissues (FFPE). Tumor DNA from FFPE samples was isolated using QIAamp DNA FFPE Tissue Kit (Qiagen, Germany). Isolated DNA samples were quantified by a Qubit 4 Fluorometer (Thermo Fisher Scientific, USA) and stored at 4°C.

DNA isolation from PBMNC samples

Mononuclear cell fraction of peripheral blood samples drawn into EDTA containing blood collection tubes was separated with Ficoll gradient centrifugation (400*g* for 30 min). Cellular DNA was extracted using the MagCore Plus II Automated Nucleic Acid Extractor (RBC Bioscience Corporation, Taiwan). Isolated DNA samples were quantified by a Qubit 4 Fluorometer (Thermo Fisher Scientific, USA) and stored at 4°C.

Droplet digital PCR

EZH2 mutation status was determined with a QX200 ddPCR system (Bio-Rad Laboratories, USA). All PCR reactions were performed using ddPCR Supermix for probes (no dUTP) (Bio-Rad Laboratories, USA) for single PCR reactions and ddPCR Multiplex Supermix (Bio-Rad Laboratories, USA) for multiplex PCR reactions. Variable amounts of mutation specific assays and 25 ng of template DNA (for all sample types, including TB, LB, and PBMNC samples) were used in each reaction. Amplification was carried out in a C1000 Touch Thermal Cycler (Bio-Rad Laboratories, USA) with a standard ddPCR protocol: 10 min at 95°C for enzyme activation, 30 s at 94°C for denaturation, and 1 min at 55°C for annealing. After 40 cycles, 98°C for 10 min was applied for enzyme inactivation. ddPCR reactions were accepted for subsequent analyses if >7000 droplets were detected. Results were analyzed and translated to copy numbers per μL values and VAF using the QuantaSoft software (version 1.7; Bio-Rad Laboratories, USA).

We set up a unique multiplex PCR scenario capable of analyzing seven *EZH2* mutation hotspots in two distinct PCR reactions. In the first PCR reaction, we used four mutation-specific (*EZH2*

p.Y646F/C/S and *EZH2* p.A682G) and two corresponding wild-type (WT) probes. In the second PCR reaction, three mutation-specific (*EZH2* p.Y646N/H and *EZH2* p.A692V) and two corresponding WT probes were used (Table S2). A TB sample was considered mutant if the detected VAF was above 1%. The *EZH2* VAF values for all BM samples were normalized for the tumor cell content using the following formula: VAF measured by ddPCR × (100/tumor content %). A VAF cutoff of 0.03% was applied for LB samples if the analytical sensitivity was below this value (determined from the measured limit of detection [LOD] values from the serial dilution experiments). Otherwise, analytical sensitivity was considered. If only one droplet was found mutant, the PCR reaction was repeated. The mean detected copy number was 333 copies/μL and 66 copies/μL for TB and LB samples, respectively. Therefore, the mean analytical sensitivity of the ddPCR reactions was 0.02% and 0.08% for TB and LB samples, respectively. This was calculated from the reciprocal sum of mutant and WT DNA fragments detected in 22 μL and multiplied by 100.

Serial dilution

A PBMNC-derived DNA mix pooled equimolarly from five healthy subjects was used to generate serial dilutions up to 100,000× from known *EZH2* mutant FFPE samples corresponding to the seven *EZH2* hotspots analyzed. To increase accuracy, additional dilution points were used (2000×, 5000×, 20,000×, and 50,000×) beside the 10-fold dilution series points (10×, 100×, 1000×, 10,000×, and 100,000×). To determine the analytical sensitivity, 100 ng DNA was used in each reaction, and PCR reactions near the sensitivity cutoff were run in triplicates for both single and multiplex ddPCR reactions.

Data analysis and statistical methods

Statistical analysis was performed using the Prism 8.0.1 software (GraphPad Software, Inc, USA). We investigated the statistical connection between *EZH2* mutation status and *EZH2* VAF levels and histological, clinical, and radiological parameters of the patients. Normal distribution of continuous variables was tested with the Shapiro–Wilk test. For the analysis of continuous variables, unpaired *T*-test, Mann–Whitney *U* test, one-way analysis of variance (ANOVA), or the Kruskal–Wallis, one-way ANOVA was used depending on the number of groups analyzed and on the distribution of variables. Categorical variables were studied with Chi-square test for trend. The interdependence of two continuous variables was tested with Pearson correlation and linear regression. Paired variables and samples were tested with paired *T*-test, Wilcoxon signed-rank test, and Friedman test depending on the number of groups analyzed and on the distribution of variables. All tests were two-sided, *p* value threshold for significance was set to 0.05%, and 95% confidence interval was applied for all analyses.

Results

EZH2 *mutation detection using a novel multiplex ddPCR assay*

First, we designed a novel multiplex droplet digital PCR approach for the simultaneous detection of distinct *EZH2* mutations. We performed a series of measurements with varying probe concentrations and combinations, resulting in an assay mix, which can stably and reproducibly detect the seven *EZH2* hotspot mutations in only two PCR reactions instead of performing seven distinct single PCR measurements (Fig. S1A,B).

We compared the LOD of single versus multiplex PCR amplifications for all *EZH2* mutations using serial dilutions. With regard to all analyzed hotspots, no statistical difference was found between the difference in the LOD of the single versus the multiplex PCR approach (paired *T*-test, $p = 0.75$). Upon analyzing all hotspots individually, we have not found a difference in the LOD for mutation-specific assays of p.Y646N/F/C/S and p.A682G. However, we detected decreased LOD for p.Y646H and p.A692V assays in the multiplex PCR setup, although neither exceeded one log difference and the analytical sensitivity remained below 0.1% for these targets as well (Table S3). Upon comparing LB- to TB-based *EZH2* analysis, we found that the LB-based approach slightly outperforms the TB-based one in terms of sensitivity and negative predictive value (NPV) (Fig. S2A,B).

EZH2 *mutation detection in TB and pretreatment LB samples*

The median isolated cfDNA yield from LB samples was 70.6 ng (range: 2–968.8 ng) per mL of initial blood plasma. *EZH2* mutations were detected in 41.5% (51/123) of the patients when considering all available sample types (diagnostic TB, relapse TB, or pretreatment LB specimen) (Fig. 1A,

Fig. 1 *(a) Enhancer of zeste homolog 2 (EZH2) mutation (MT) status in all investigated samples. (b) EZH2 MT status in patients with paired tissue (TB) and pretreatment liquid biopsy (LB) samples. Patients harboring mutation exclusively in one compartment (TB or LB only) are displayed individually. (c) Variant allele frequencies (VAF) in EZH2 mutant patients with paired TB and pretreatment LB samples. VAFs are displayed on a log2 scale.*

Table S4). Analyzing the paired TB–LB samples (n = 114), the *EZH2* mutation frequency was 37.8% (43/114), and it did not differ significantly between the TB and the LB samples (29.9% vs. 32.5%, respectively, Chi-square test, p = 0.67). However, in six patients (5.3%), the *EZH2* mutation was detected exclusively in the TB samples, whereas in nine (7.9%) patients, the *EZH2* mutation was only detected in the corresponding LB sample (Fig. 1B,C, Table S4). The *EZH2* frequency in patients with paired TB–LB (n = 78) samples at diagnosis proved to be 37.1% (29/78). In the cohort of patients with paired TB and LB samples, 51 different mutations were found in 43 patients. Among these 51 mutations, 28 mutations were present in both compartments, whereas 9 and 14 were only present in the TB or in the LB, respectively (Fig. 2).

With a median follow-up time of 29 months (range: 6–229), 50 patients (39.7%) relapsed after treatment or progressed after at least 12 months of watch and wait approach. From these 50 patients, 39 had an *EZH2* mutation analysis both at the time of diagnosis and relapse/disease progression from at least 1 sample. We observed a switch in the *EZH2* mutation status during the disease course in 14 patients (35.9%) who had paired diagnostic and relapse samples available (Fig. 3A,B). In four patients with paired diagnostic and relapse TB, the measured *EZH2* VAF significantly increased at the time of relapse (paired T-test, p = 0.02, Fig. 3C). Altogether, 51.3% of relapsed patients in this cohort harbored an *EZH2* mutation at one point during the disease course (Fig. 3A,B).

The spectrum of *EZH2* mutations in diagnostic and relapse TB samples is summarized in Fig. 4A,B. We found a relative increase in the proportion of p.Y646N and decrease in the proportion of p.Y646F and p.Y646H mutations at the time of relapse. Median *EZH2* mutation VAF was 21.8% (range 1.0%–54.6%) and 2.3% (range 0.1%–74%) in TB samples and in pretreatment LB samples, respectively (Fig. 5A,B).

Multiple TB samples collected at the same time from distinct sites were available from 54 patients. Spatial heterogeneity was documented in eight patients (15%), in cases where different *EZH2* mutation types were detected in distinct sites, or in patients with at least one mutant and one WT tumor site (Fig. 2, Table S4). Intra-tumoral heterogeneity (multiple *EZH2* mutations within a single TB sample) was identified in 5.4% (3/56) of all nodal mutant TB samples (Table S4). Multiple *EZH2* mutations were found in 14% of pretreatment LB samples (6/43) reflecting inter-tumoral spatial heterogeneity (Fig. 2). For example, in Pt-38, two distinct *EZH2* mutations (p.Y646C and p.Y646N) were detected in the LB specimen. However, only the *EZH2* p.Y646C mutation was detected in the cervical lymph node biopsy. Moreover, this patient had a large retroperitoneal and mediastinal mass on PET/CT, which raises the possibility that the *EZH2* p.Y646N mutant clone was restricted to those sites (Fig. 6).

Correlation of EZH2 *mutation status and VAF levels with histological, clinical, and radiological parameters*

Detailed patient characteristics stratified by *EZH2* mutation status at the time of diagnosis are displayed in Table S5. Altogether, we analyzed 215 TB samples collected from 122 patients at the time of diagnosis or at relapse. We found a trend between higher histological grade and mutant TB *EZH2* status (Chi-square test, p = 0.1) and LB *EZH2* VAF level (Mann–Whitney U test, p = 0.08) (Fig. 7A,B). In addition, we found a significant association between TB grade and higher TB *EZH2* VAF level (unpaired T-test, p = 0.009) (Fig. 7C). We also found a significant connection between TB *EZH2* VAF and LB *EZH2* VAF levels (linear regression, p = 0.048) (Fig. S3A).

Interestingly, we found that WT *EZH2* status may be associated with increased risk of BM infiltration, although this did not reach statistical significance (Chi-square test, p = 0.1). However, histologically confirmed BM infiltrates (with a median 17.5% infiltration by tumor cells) were more frequently *EZH2* WT, regardless of the mutation status of the paired TB: only 6 out of the 10 patients with paired mutant TB displayed an *EZH2* mutation in the BM as well. On the contrary, only one patient harbored an *EZH2* mutation in the BM among the 34 patients with paired WT TB (Fig. 7D, Table S6). Altogether, 16% (7/44) of infiltrated BM samples harbored the mutation. Meanwhile, 84% (37/44) proved to be *EZH2* WT.

There was no difference between median *EZH2* VAF at the time of diagnosis and progression/relapse (2.6% vs. 8%, Mann–Whitney U test, p = 0.09). Importantly, we found a statistically nonsignificant trend between LB *EZH2* VAF levels and Follicular

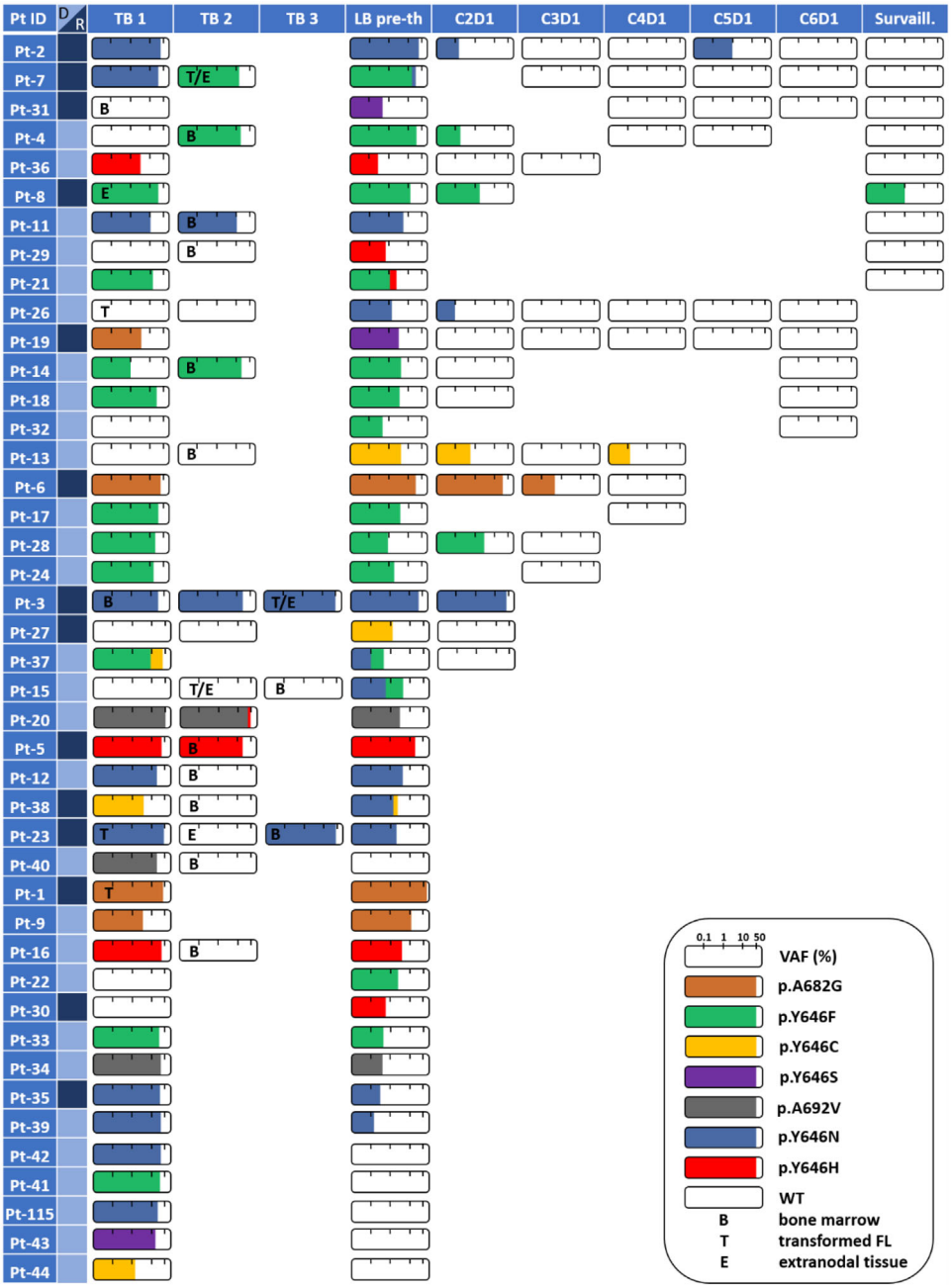

Fig. 2 *Enhancer of zeste homolog 2 (EZH2) mutation pattern in 43 mutant follicular lymphoma patients with paired tissue (TB) and liquid biopsy samples (LB). Saturation of the bars represents variant allele frequencies (VAF) in a log2 scale. EZH2 VAFs (range: 0.1%–74.0%) were multiplied by 100 (to avoid zero and minus values) then transformed to a log2 scale. Subsequently, each value was converted to percentage for illustration, where 100% VAF would occur as a fully saturated bar. C2D1, cycle 2 day 1; C3D1, cycle 3 day 1; C4D1, cycle 4 day 1; C5D1, cycle 5 day 1; C6D1, cycle 6 day 1; D, diagnosis; Pre-th, pretreatment; R, relapse; Surveill, surveillance sample (LB sample collected after therapy); WT, wild-type.*

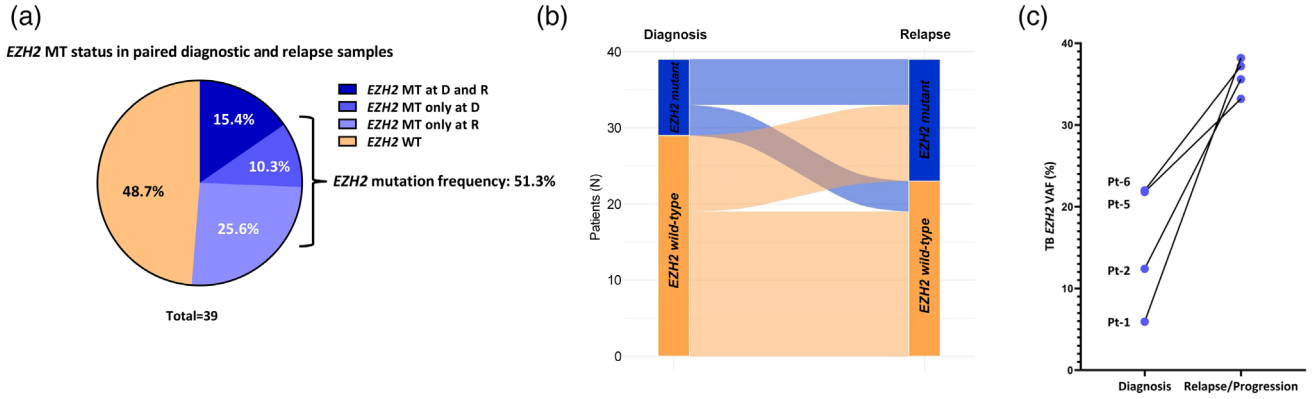

Fig. 3 *(A) Combined enhancer of zeste homolog 2 (EZH2) mutation frequency in patients with paired diagnostic and relapse samples. (B) EZH2 mutation status switch phenomenon in patients with paired diagnostic and relapse sample. Alluvial plot was created using the ggalluvial package (version 0.12.3) (10.21105/joss.02017) in the R statistical environment version 4.2.2 (R Core Team, R Foundation for Statistical Computing, Vienna, Austria). C: Comparison of EZH2 VAFs between diagnosis and relapse in four patients with paired mutant TBs.*

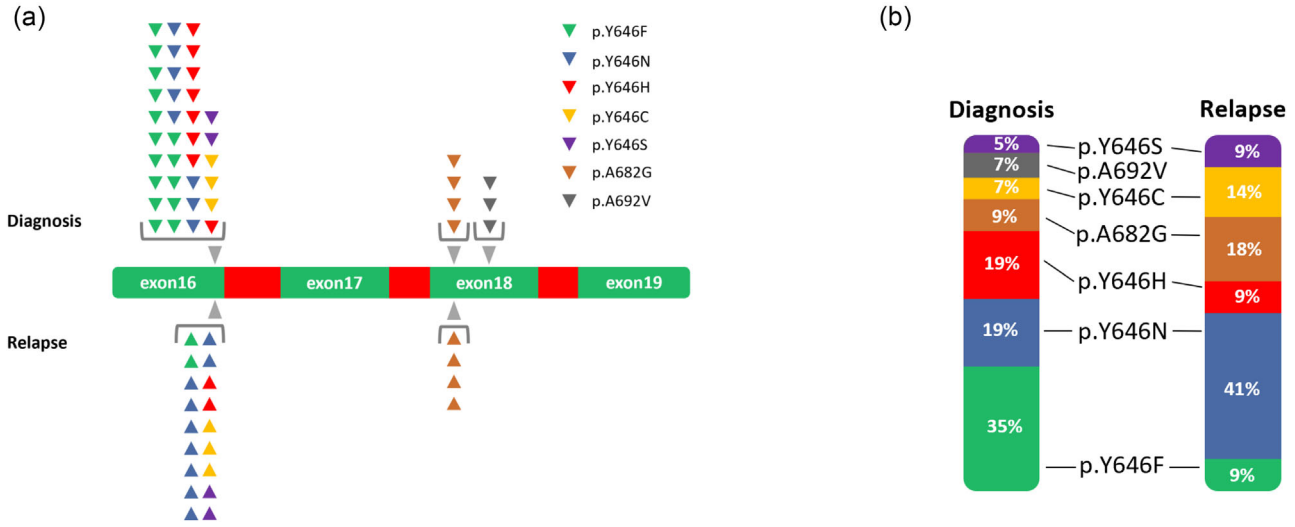

Fig. 4 *(A) Distribution of SET domain enhancer of zeste homolog 2 (EZH2) mutation types in samples collected at the time of diagnosis (n = 43) and at relapse (n = 22). The type of EZH2 mutation did not change in patients with paired mutant diagnostic and relapsed samples (n = 6) between the two timepoints. (B) The bar graphs show the distribution of EZH2 mutation types at the time of diagnosis (n = 43) and at relapse (n = 22). The percentages in the bar graphs represent the ratio of a particular mutation at diagnosis or at relapse.*

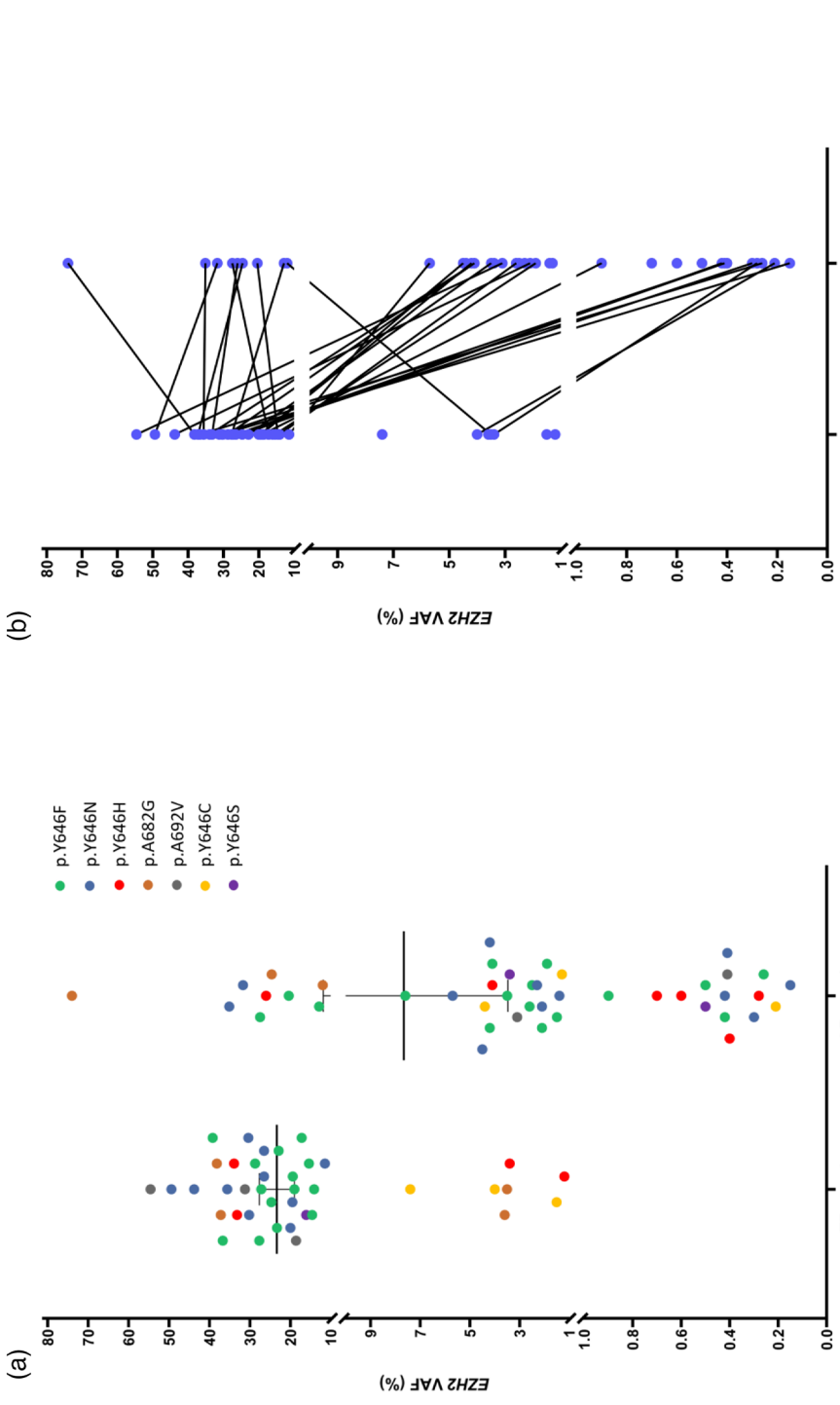

Fig. 5 *(A) Comparison of enhancer of zeste homolog 2 (EZH2) mutation types detected in tissue (TB) and liquid biopsy (LB) samples. (B) Comparison of EZH2 variant allele frequencies (VAF) between paired TB and LB samples in EZH2 mutant patients.*

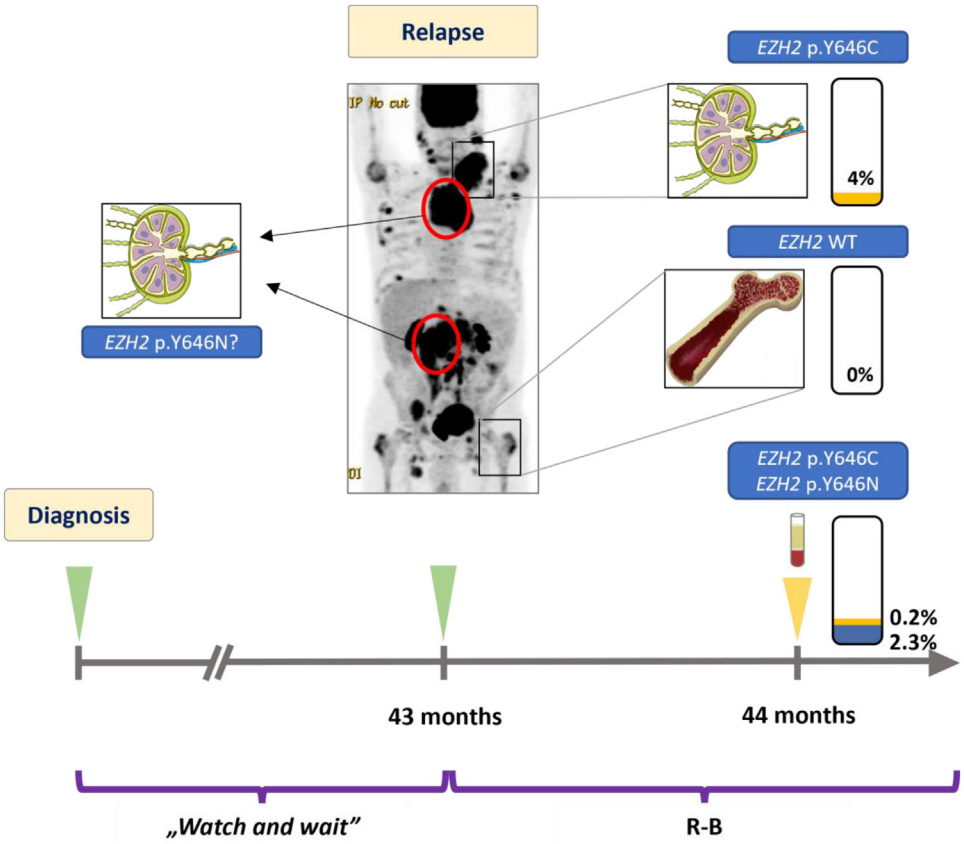

Fig. 6 *In the case of Pt-38, a subclonal enhancer of zeste homolog 2 (EZH2) mutation was found in the TB at the time of relapse, with an additional EZH2 mutation present in the paired liquid biopsy sample. Extensive involvement of the mediastinal and retroperitoneal region was found on imaging, in which unbiopsied regions may have been the source of the additional p.Y646N mutation found only in the peripheral blood.*

Lymphoma International Prognostic Index (FLIPI) score (Fig. 7E), LDH levels (Fig. S3B), bulky disease (Fig. S3C), presence of extranodal disease (Fig. S3D), and clinical stage (Fig. S3E). The presence of B symptoms was significantly (Chi-square test, $p = 0.045$) associated with mutant *EZH2* status (Fig. 7F).

EZH2 *mutation detection in longitudinally collected follow-up LB samples*

Follow-up LB samples collected on the first day of at least two of each treatment cycle were available from 19 patients. Four additional patients were also analyzed with pre- and posttreatment (surveillance) samples (Table S8). Median *EZH2* VAF was 3.5% and 0.12% before treatment and at the time of C2D1, respectively (Fig. 8A, Table S8). The difference between C1D1 and C2D1 VAF was not significant (Wilcoxon signed-rank test, $p = 0.06$, Table S7), although we observed a strong correlation upon analyzing those patients who responded to immune-chemotherapy (Wilcoxon signed-rank test, $p = 0.005$) (Fig. 8B, Table S7). *EZH2* VAF significantly decreased at the beginning of all subsequent cycles compared to C1D1 (Fig. 8A) (Table S6). Patients responding to therapy were characterized by a prompt decrease in the *EZH2* VAF level after the initiation of treatment. Meanwhile, this did not happen in Pt-3, Pt-6, and Pt-28 who initially did not show clinical response (Fig. 8C). Pt-6, at the time of relapse, was first treated with R-CVP (rituximab plus cyclophosphamide, vincristine, and prednisone) and showed no improvement in clinical symptoms after two cycles; therefore, the therapy was intensified to R-CHOP (rituximab plus cyclophosphamide, doxorubicin, vincristine, and prednisone combination), and a prompt response

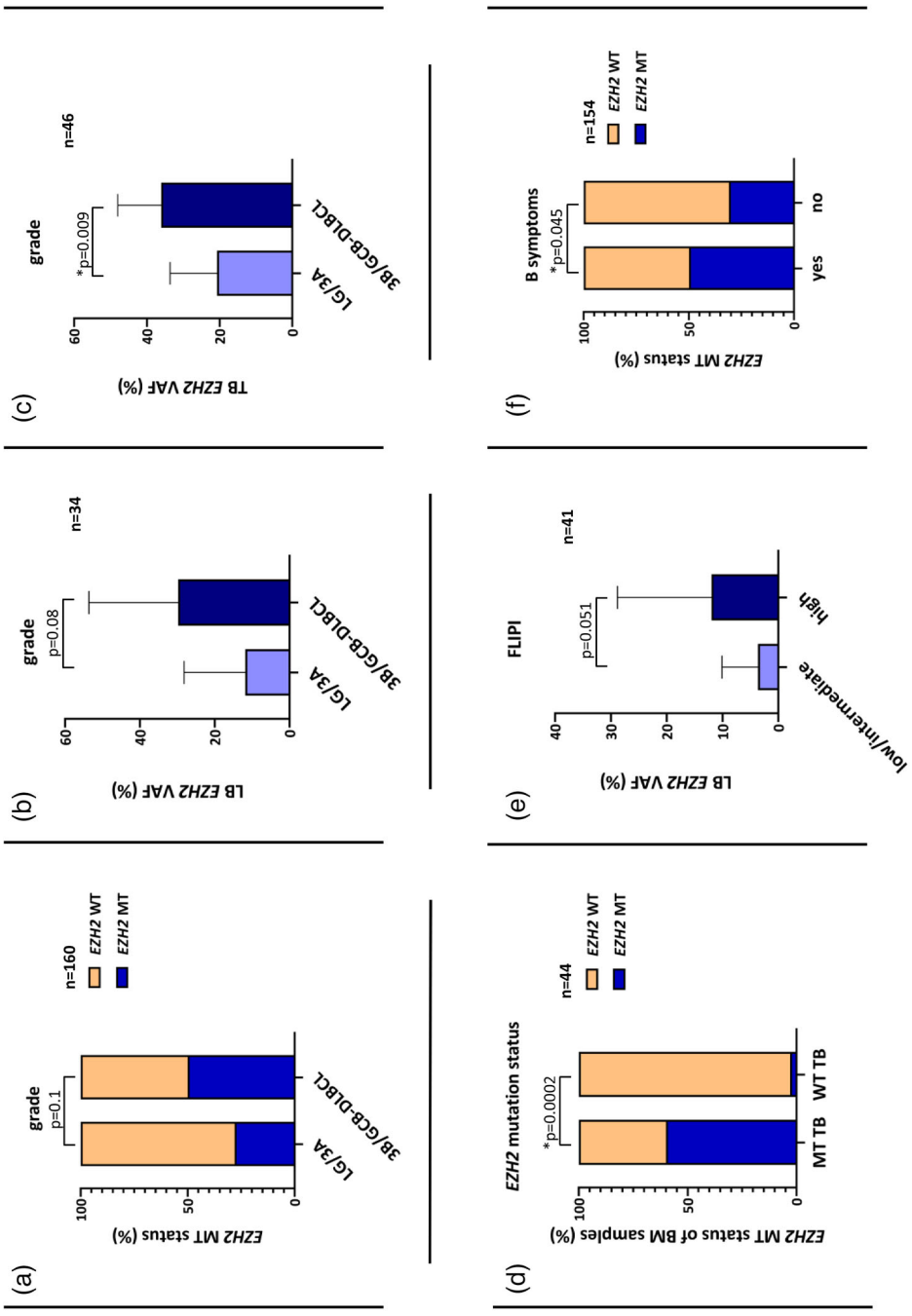

Fig. 7 *Correlation among enhancer of zeste homolog 2 (EZH2) mutation status, EZH2 variant allele frequencies (VAF), and histological and clinical variables. (A) Percentage of EZH2 mutant follicular lymphoma (FL) cases in each histological FL grade group. (B) Association between pretreatment liquid biopsy (LB) EZH2 variant allele frequency (VAF) levels and tissue biopsy (TB) histology grade. If a patient had more than one mutant TB at the same time, the higher histological grade was considered. (C) Relationship between tissue biopsy (TB) EZH2 VAF and histological grade. (D) Association between the EZH2 mutation status of histology confirmed FL infiltrated bone marrow (BM) biopsy and the EZH2 mutation status of paired corresponding TB (lymph node or extranodal) sample. (E): Connection between pretreatment LB EZH2 VAF and Follicular Lymphoma International Prognostic Index (FLIPI) score. (F) Proportion of EZH2 mutations in patients with or without B symptoms. GCB-DLBCL, germinal center B-cell like diffuse large B-cell lymphoma; LG, low grade; MT, mutant; WT, wild-type.*

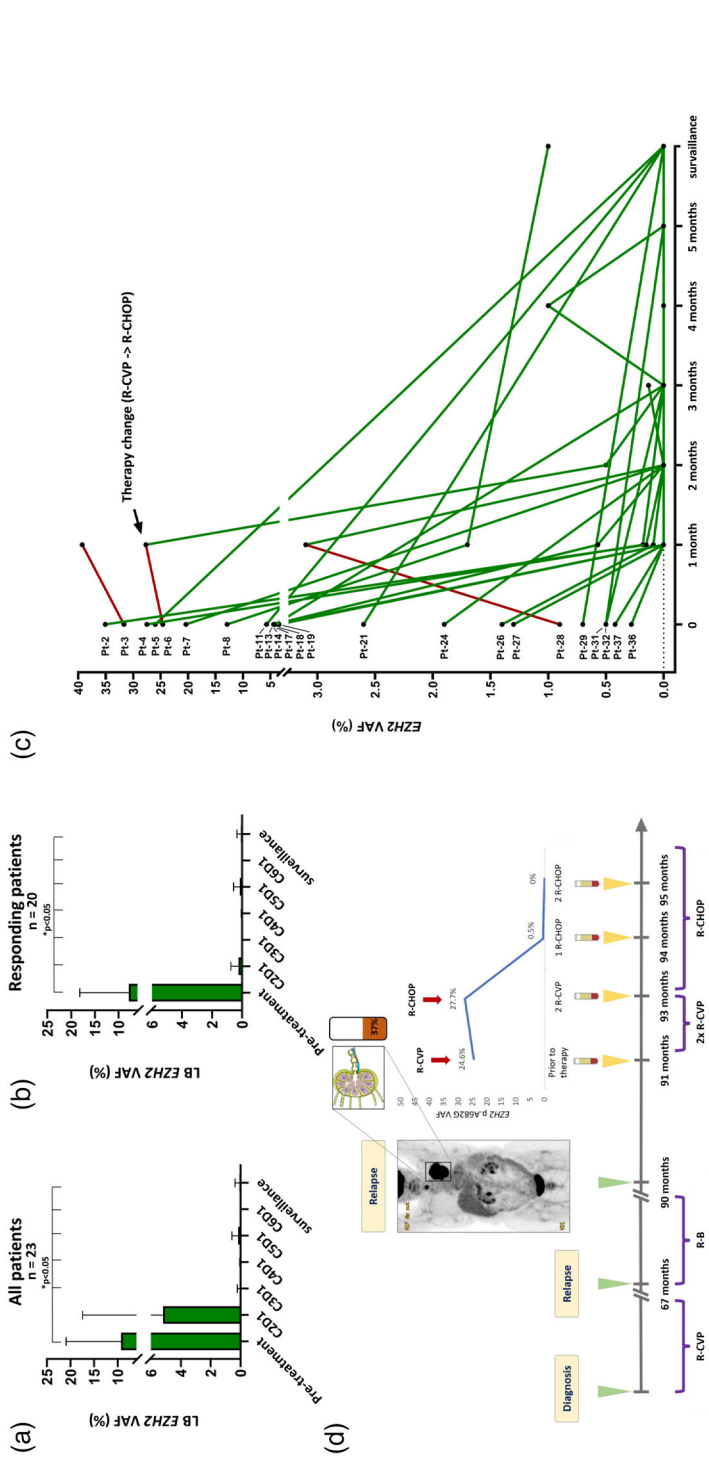

Fig. 8 *Enhancer of zeste homolog 2 (EZH2) mutation analysis in longitudinally collected follow-up liquid biopsy samples. (A) Median EZH2 variant allele frequencies (VAF) before each treatment cycle in all patients. (B) Median EZH2 variant allele frequencies (VAF) before each treatment cycle in patients responding to therapy. (C) Spider plot showing alterations in liquid biopsy (LB) EZH2 VAFs in response to therapy in patients with follow-up LB samples. X axis represents elapsed time from the initiation of treatment in months. Patients without clinical response are labeled with red. All 23 patients had available LB sample at C1D1. Among these 23 patients, 61%, 39%, 39%, 26%, 35%, and 52% had an LB sample at the time of C2D1, C3D1, C4D1, C5D1, C6D1 and at a surveillance timepoints, respectively. (D) Illustration of temporal changes in EZH2 VAFs in response to therapy in the case of Pt-6. C1D1, cycle 1 day 1; C2D1, cycle 2 day 1; C3D1, cycle 3 day 1; C4D1, cycle 4 day 1; C5D1, cycle 5 day 1; C6D1, cycle 6 day 1; R-B, rituximab plus bendamustine; R-CHOP, rituximab plus cyclophosphamide, doxorubicin, vincristine and prednisone; R-CVP, rituximab plus cyclophosphamide, vincristine, and prednisone.*

was registered clinically and molecularly as well (Fig. 8D).

Surveillance LB sampling provided proof-of-concept for early relapse detection in the case of Pt-118, who experienced *EZH2* mutant relapse 1 year after rituximab monotherapy, where *EZH2* p.Y646N mutation was detected in the LB specimen. Interestingly, the same *EZH2* p.Y646N with low VAF was detected 6 months before the clinical relapse in a surveillance LB sample (Fig. S4).

Comparison of EZH2 *mutation analysis in LB and PBMNC specimens*

We tested the *EZH2* mutation status of PBMNC samples of patients whose LB sample carried an *EZH2* mutation (Table S9). Fifty-three paired PBMNC and LB samples were available for analysis with only 17/53 (32%) PBMNC samples carrying the *EZH2* mutation detected in the corresponding LB sample (Fig. S5). Interrogating these 17 samples, *EZH2* VAF was significantly higher in the LB samples compared to the corresponding PBMNC samples (mean VAF: 5.7% vs. 0.04%, Wilcoxon signed-rank test, $p < 0.0001$) (Fig. S5).

Discussion

In this study, we performed an in-depth spatio-temporal analysis of *EZH2* mutations in FL using tissue- and liquid biopsy samples, and we identified gain-of-function mutations in a considerably higher proportion of patients than previously reported in studies focusing on single-tissue biopsies.

Tazemetostat—a novel, orally active inhibitor of EZH2—was recently approved in the United States for relapsed or refractory *EZH2* mutant FL patients who received at least two prior systemic therapies and for patients who have no satisfactory alternative treatment options, regardless of their *EZH2* mutation status [21]. The approval was based on a phase 2, multicenter, single-arm clinical study, in which the objective response rate to single-agent tazemetostat in a pretreated cohort was found to be 69% and 35% in *EZH2* mutant and WT FL patients, respectively. In a preliminary communication of this study, the authors highlighted that the presence of *EZH2* mutation was the only predictor of response in both TB and LB in patients with FL [37]. It is also worth noting that around one third of patients with WT *EZH2* also showed a response to the treatment. In this study, we developed a novel, LB-based *EZH2* mutation-detection assay, which revealed a substantially higher *EZH2* mutation frequency in a heterogeneous cohort of untreated and relapsed/progressed FL patients. This observation, in addition to (epi)genetic alterations and microenvironmental factors, may also explain at least a proportion of the unanticipated response to tazemetostat monotherapy in 35% of the *EZH2* WT subcohort of the phase 2 study.

EZH2 gain-of-function hotspot mutations in exons 16 and 18 were discovered by Morin et al. [38, 39]. Subsequently, *EZH2* mutation frequency in FL was described to be 12% by Sanger sequencing [40]. More sensitive NGS-based methods later revealed that 20%–27% of FL patients harbor these mutations [4, 13, 15, 17]. The largest published cohort of nearly 600 patients so far has confirmed these results [14]. However, these studies relied on single-site tissue biopsies obtained at single timepoints that may not represent the indolent systematic disease.

In this study, we report *EZH2* mutations in 37.8% of the 117 paired TB and LB samples with a mutation frequency of 41.5% in the whole cohort of 123 FL patients. The higher mutation frequency in our cohort can be explained by two reasons: (i) the acquisition of *EZH2* mutations during the disease course as a result of temporal evolution and (ii) spatial heterogeneity in clonal processes leading to different clonal compositions both within one tumor site and between different tumor sites.

First, supporting the consideration of temporal evolution in the evaluation of *EZH2* mutation status, our cohort contains 39 FL patients with paired *EZH2* analysis at diagnosis and relapse, where we report *EZH2* mutation status class switch (including both gain and loss) in 35.9% of cases. This data demonstrates that *EZH2* mutation status can dynamically change throughout the disease course and may exhibit significant clonal tiding. Therefore, *EZH2* mutation frequency in FL can be underestimated if not analyzed temporally before each therapy line.

A second explanation for the higher *EZH2* mutation prevalence documented in this study is the phenomenon of spatial heterogeneity. Here, we report nine patients in which *EZH2* mutations were exclusively detected in the plasma specimen. These patients harbored a median 5 (range 2–10),

metabolically active, unbiopsied tumor region by PET/CT, which may indeed represent the origin of the *EZH2* mutant ctDNA fragments detected in LB samples. This finding underlines the value of LB in capturing genetic information blinded to random single-site biopsies. Analyzing paired LB and TB samples, 8%–50% of all detected mutations were found only in the ctDNA compartment in studies investigating Hodgkin lymphomas (HL) or DLBCLs [25, 41–45]. In a recent study using targeted sequencing, 8% of all mutations were exclusively found only in the LB specimen of FL patients [46]. In our study, interrogating only a single gene in patients with paired TB–LB biopsies, the proportion of patients in which *EZH2* mutation was exclusively identified in the blood plasma was 7.9%. Moreover, 27.5% (14/51) of *EZH2* mutations were exclusively found in the LB specimen, most likely as a result of spatial heterogeneity.

Of note, we could not detect *EZH2* mutation in the LB specimen of six patients, albeit the paired TB sample proved to be *EZH2* mutant. This observation is in line with the reported result of Fernández-Miranda et al., in which 25% of all mutations were only found in the TB specimen of FL patients [46]—whereas in our study, 17% of all *EZH2* mutations were not detected in the peripheral blood. Pt-44 carried a subclonal mutation (1.51%) in the TB sample, most likely explaining the *EZH2* WT status in the LB sample. However, the discordant mutation status could not be explained by histological, clinical, molecular, and radiological data in patients Pt-40, Pt-41, Pt-42, Pt-43, and Pt-115. The lower cfDNA yield may theoretically explain the discordant mutation status in the remaining LB samples with mutant corresponding TB samples. However, these LB samples did not differ considerably in their quantity and QC metrics from the cases with concordant LB–TB mutation status. Based on this data, the NPV of our LB-based approach is 92%, and the specificity is 89%. These results show that LB analysis alone may not always be sufficient in detecting disease-specific biomarkers. However, one has to emphasize that the statistical sensitivity and the NPV of the LB-based mutation analysis were found to be superior compared to TB-based analysis. According to our results, the best sensitivity for *EZH2* mutation analysis can be achieved with the parallel investigation of TB and LB samples, which may represent the future optimal screening strategy for *EZH2* mutations in routine clinical practice before treatment lines where the usage of targeted therapy is considered. We envision that LB-based analysis would be strongly advised in cases with advanced disease and high tumor burden and in cases with hard-to-biopsy tumor sites (e.g., central nervous system and retroperitoneal involvement).

Huet et al. reported an inverse correlation between *EZH2* alterations (mutation and amplification) and B symptoms and rate of BM infiltration in FL [47]. Here, we also observed an association between *EZH2* mutant FL and lack of BM infiltration. When analyzing paired lymph node and BM biopsies, we found that the *EZH2* WT FL clone may be more prone to infiltrate the BM compared to the *EZH2* mutant clone. These findings raise the idea that the lack of *EZH2* mutation in FL may be a biomarker indicating an increased risk of BM infiltration. However, this needs to be confirmed in larger cohorts. In contrast to the observations by Huet et al., we detected a significant association between the presence of *EZH2* mutations and B symptoms.

Tumor burden is an established prognostic factor in lymphomas. Therefore, there is a great clinical need for methods accurately measuring this parameter. The increased metabolic activity characteristic of aggressive lymphomas is usually accompanied by increased ctDNA excretion to the blood [26]. In line with this, here we report a trend between LB *EZH2* VAF levels and more aggressive histology. In DLBCL and HL, it is also well documented that pretreatment ctDNA levels independently mirror distinct parameters that indicate tumor burden (international prognostic index, LDH level, stage, and total metabolic tumor volume [TMTV]) [29, 41, 42, 48]. In FL, TMTV is the only parameter that has been independently linked to LB ctDNA abundance [33, 49, 50]. However, only limited and controversial results are available in connection with other indexes [46, 50]. We did not find a significant correlation between LB *EZH2* VAF levels and basic clinical parameters, although we found a trend with FLIPI, LDH levels, bulky disease, presence of extranodal involvement, and clinical stage. The nonsignificant associations may be explained by the relatively small number of investigated patients with *EZH2* mutation in the plasma ($n = 41$), so that sample size may not be enough to uncover statistically significant associations in an indolent lymphoma. Moreover, the investigation of a single gene may not accurately represent the total amount of ctDNA molecules in the plasma with a genetically diverse disease such as FL.

Undetectable ctDNA, or at least a 100-fold reduction in ctDNA levels after 2 cycles of therapy, indicates excellent treatment response and outcome in DLBCL, HL, and mantle cell lymphoma (MCL) [28, 42, 51, 52]. Here, we found a significant drop (>100-fold) in the *EZH2* levels after two cycles of immunochemotherapy comparing pretreatment and C3D1 levels. No statistical difference was observed between pretreatment and C2D1 timepoints regarding all patients. However, statistical difference was detected between pretreatment and C2D1 levels when restricting the analysis to the responding patients, indicating that the investigation of LB samples may mirror early therapeutic response in FL, and that dynamic monitoring of ctDNA levels might have similar clinical value as in DLBCL or in HL. The case of Pt-6 in our study, in which initial refractoriness to R-CVP was followed by a prompt decrease in the *EZH2* VAF level after initiation of R-CHOP, demonstrates that ctDNA-based monitoring offers a real-time, radiation-free disease monitoring alternative in FL as well. During surveillance, in the majority of DLBCL and MCL cases, signs of lymphoma recurrence can be detected with a 3–7-month lead time with LB analysis [48, 52, 53]. To the best of our knowledge, no data is available in the context of minimal residual disease detection using ctDNA in FL. Here, we demonstrate an FL case (Pt-118) where mutant *EZH2* ctDNA fragments could be detected during surveillance, 6 months prior to the clinical relapse, harboring an identical *EZH2* mutation within the relapse sample. This case indicates that LB-based monitoring of FL may be valuable in predicting future relapses.

The majority of the studies in the last three decades published on the minimally invasive detection and monitoring of FL focus on the interrogation of *BCL2/IGH* translocation or the clonal V(D)J rearrangements from PBMNCs [35, 54, 55]. To date, no one has directly compared the value of the cellular and acellular compartment of the peripheral blood in FL for molecular analysis. Here, we show that mutant *EZH2* DNA fragments can be more sensitively detected from ctDNA compared to PBMNCs. In our cohort, the majority of PBMNC samples with paired mutant LB samples lacked *EZH2* mutation. Moreover, the *EZH2* VAF values in *EZH2* mutant PBMNCs were substantially lower compared to the corresponding LB samples. This supports the theory that ctDNA may be more reliable in detecting traits of the disease compared to PBMNC-based methods in FL.

Conclusions

In this study, we developed a highly sensitive novel *EZH2* mutation detection approach applicable to LB specimens as well as classical TB samples. Owing to the temporal analysis of paired diagnostic and relapse samples and due to the ability of this approach to resolve spatial heterogeneity, our method detected a higher frequency of *EZH2* mutations in FL patients compared to historical data (37% vs. 27% at diagnosis). This result may further expand the subset of FL patients who would most likely benefit from the recently approved EZH2 inhibitor targeted therapy.

Author contributions

Conceptualization; data curation; formal analysis; funding acquisition; investigation; methodology; project administration; resources; validation; visualization; writing—original draft: Ákos Nagy. *Conceptualization; data curation; formal analysis; investigation; methodology; project administration; resources; supervision; validation; visualization; writing—review and editing*: Bence Bátai. *Investigation; methodology; project administration; validation; visualization; writing—review and editing*: Laura Kiss. *Investigation; methodology; writing—review and editing*: Stefánia Gróf. *Data curation; writing—review and editing*: Péter Attila Király, Ádám Jóna, Hermina Sánta, Piroska Pettendi, Tamás Szendrei, Márk Plander, and Gábor Körösmezey. *Writing—review and editing*: Judit Demeter, Árpád Bátai, Hussain Alizadeh, Béla Kajtár, Gábor Méhes, László Krenács, Erika Tóth, Tamás Schneider, Gábor Mikala, and András Masszi. *Investigation; writing—review and editing*: Botond Timár and Judit Csomor. *Funding acquisition; writing—review and editing*: András Matolcsy and Donát Alpár. *Conceptualization; funding acquisition; resources; supervision; visualization; writing—review and editing*: Csaba Bödör.

Conflict of interest statement

The authors declare that they have no conflict of interests.

Funding information

Prepared with the support of the H2020 (SGA No. 739593) grant of the European Union, the Doctoral Student Scholarship (NKFIH KDP-1022882) of the Cooperative Doctoral Program of the Ministry of Innovation and Technology, the Semmelweis 250+ Excellence Ph.D. Scholarship from the

EFOP-3.6.3-VEKOP-16-2017-00009 grant, New National Excellence Program of the Ministry for Innovation and Technology (ÚNKP-21-3-II-SE-24, ÚNKP-22-5-SE-7), the Hungarian National Research, Development and Innovation Office (NKFIH K21-137948, FK20_134253), the Higher Education Institutional Excellence Program of the Ministry of Human Capacities in Hungary (TKP2021-EGA-24 and TKP2021-NVA-15), and the János Bolyai Research Scholarship program (ID: BO/00125/22) of the Hungarian Academy of Sciences and Elixir Hungary.

References

1 Teras LR, DeSantis CE, Cerhan JR, Morton LM, Jemal A, Flowers CR. 2016 US lymphoid malignancy statistics by World Health Organization subtypes. *CA Cancer J Clin.* 2016;**66**:443–59.
2 Carbone A, Roulland S, Gloghini A, Younes A, von Keudell G, Lopez-Guillermo A, Fitzgibbon J. Follicular lymphoma. *Nat Rev Dis Primers.* 2019;**5**:83.
3 Link BK, Maurer MJ, Nowakowski GS, Ansell SM, Macon WR, Syrbu SI, et al. Rates and outcomes of follicular lymphoma transformation in the immunochemotherapy era: a report from the University of Iowa/Mayo Clinic specialized program of research excellence molecular epidemiology resource. *J Clin Oncol.* 2013;**31**:3272–8.
4 Okosun J, Bodor C, Wang J, Araf S, Yang CY, Pan C, et al. Integrated genomic analysis identifies recurrent mutations and evolution patterns driving the initiation and progression of follicular lymphoma. *Nat Genet.* 2014;**46**:176–81.
5 Pasqualucci L, Khiabanian H, Fangazio M, Vasishtha M, Messina M, Holmes AB, et al. Genetics of follicular lymphoma transformation. *Cell Rep.* 2014;**6**:130–40.
6 Kridel R, Chan FC, Mottok A, Boyle M, Farinha P, Tan K, et al. Histological transformation and progression in follicular lymphoma: a clonal evolution study. *PLoS Med.* 2016;**13**:e1002197.
7 Bouska A, Zhang W, Gong Q, Iqbal J, Scuto A, Vose J, et al. Combined copy number and mutation analysis identifies oncogenic pathways associated with transformation of follicular lymphoma. *Leukemia.* 2017;**31**:83–91.
8 Krysiak K, Gomez F, White BS, Matlock M, Miller CA, Trani L, et al. Recurrent somatic mutations affecting B-cell receptor signaling pathway genes in follicular lymphoma. *Blood.* 2017;**129**:473–83.
9 Gonzalez-Rincon J, Mendez M, Gomez S, García JF, Martín P, Bellas C, et al. Unraveling transformation of follicular lymphoma to diffuse large B-cell lymphoma. *PLoS One.* 2019;**14**:e0212813.
10 Korfi K, Ali S, Heward JA, Fitzgibbon J. Follicular lymphoma, a B cell malignancy addicted to epigenetic mutations. *Epigenetics.* 2017;**12**:370–7.
11 Rosenquist R, Bea S, Du MQ, Nadel B, Pan-Hammarstrom Q. Genetic landscape and deregulated pathways in B-cell lymphoid malignancies. *J Intern Med.* 2017;**282**:371–94.
12 Buhler MM, Martin-Subero JI, Pan-Hammarstrom Q, Campo E, Rosenquist R. Towards precision medicine in lymphoid malignancies. *J Intern Med.* 2022;**292**:221–42.
13 Pastore A, Jurinovic V, Kridel R, Hoster E, Staiger AM, Szczepanowski M, et al. Integration of gene mutations in risk prognostication for patients receiving first-line immunochemotherapy for follicular lymphoma: a retrospective analysis of a prospective clinical trial and validation in a population-based registry. *Lancet Oncol.* 2015;**16**:1111–22.
14 Okosun J, Bödör C, Batlevi C, Nagy N, Michot J, Schneider T, et al. EZH2 gain-of-function mutations are not associated with more favorable prognosis in relapsed/refractory follicular lymphoma (FL): a preliminary analysis on 590 patients. *Hematol Oncol.* 2019;**37**:192–3.
15 Bodor C, Grossmann V, Popov N, Okosun J, O'riain C, Tan K, et al. EZH2 mutations are frequent and represent an early event in follicular lymphoma. *Blood.* 2013;**122**:3165–8.
16 Davis AR, Stone SL, Oran AR, Sussman RT, Bhattacharyya S, Morrissette JJD, Bagg A. Targeted massively parallel sequencing of mature lymphoid neoplasms: assessment of empirical application and diagnostic utility in routine clinical practice. *Mod Pathol.* 2021;**34**:904–21.
17 Garcia-Alvarez M, Alonso-Alvarez S, Prieto-Conde I, Jiménez C, Sarasquete ME, Chillón MC, et al. Genetic complexity impacts the clinical outcome of follicular lymphoma patients. *Blood Cancer J.* 2021;**11**:11.
18 Morin RD, Arthur SE, Assouline S. Treating lymphoma is now a bit EZ-er. *Blood Adv.* 2021;**5**:2256–63.
19 Morschhauser F, Tilly H, Chaidos A, Mckay P, Phillips T, Assouline S, et al. Tazemetostat for patients with relapsed or refractory follicular lymphoma: an open-label, single-arm, multicentre, phase 2 trial. *Lancet Oncol.* 2020;**21**:1433–42.
20 von Keudell G, Salles G. The role of tazemetostat in relapsed/refractory follicular lymphoma. *Ther Adv Hematol.* 2021;**12**:20406207211015882.
21 United States Food and Drug Administration. FDA granted accelerated approval to tazemetostat for follicular lymphoma. Available online: https://www.fda.gov/drugs/fda-granted-accelerated-approval-tazemetostat-follicular-lymphoma
22 Haebe S, Shree T, Sathe A, Day G, Czerwinski DK, Grimes SM, et al. Single-cell analysis can define distinct evolution of tumor sites in follicular lymphoma. *Blood.* 2021;**137**:2869–80.
23 Araf S, Wang J, Korfi K, Pangault C, Kotsiou E, Rio-Machin A, et al. Genomic profiling reveals spatial intra-tumor heterogeneity in follicular lymphoma. *Leukemia.* 2018;**32**:1261–5.
24 Huet S, Salles G. Potential of circulating tumor DNA for the management of patients with lymphoma. *JCO Oncol Pract.* 2020;**16**:561–8.
25 Rossi D, Diop F, Spaccarotella E, Monti S, Zanni M, Rasi S, et al. Diffuse large B-cell lymphoma genotyping on the liquid biopsy. *Blood.* 2017;**129**:1947–57.
26 Schroers-Martin JG, Kurtz DM, Soo J, Jin M, Scherer F, MPhil AC, et al. Determinants of circulating tumor DNA levels across lymphoma histologic subtypes. *Blood.* 2017;**130**:4018.
27 Camus V, Sarafan-Vasseur N, Bohers E, Dubois S, Mareschal S, Bertrand P, et al. Digital PCR for quantification of recurrent and potentially actionable somatic mutations in circulating free DNA from patients with diffuse large B-cell lymphoma. *Leuk Lymphoma.* 2016;**57**:2171–9.
28 Kurtz DM, Soo J, Co Ting Keh L, Alig S, Chabon JJ, Sworder BJ, et al. Enhanced detection of minimal residual disease by targeted sequencing of phased variants in circulating tumor DNA. *Nat Biotechnol.* 2021;**39**:1537–47.

29 Scherer F, Kurtz DM, Newman AM, Stehr H, Craig AFM, Esfahani MS, et al. Distinct biological subtypes and patterns of genome evolution in lymphoma revealed by circulating tumor DNA. *Sci Transl Med.* 2016;**8**:364ra155.
30 Ansell SM, Armitage JO. Positron emission tomographic scans in lymphoma: convention and controversy. *Mayo Clin Proc.* 2012;**87**:571–80.
31 Han HS, Escalon MP, Hsiao B, Serafini A, Lossos IS. High incidence of false-positive PET scans in patients with aggressive non-Hodgkin's lymphoma treated with rituximab-containing regimens. *Ann Oncol.* 2009;**20**:309–18.
32 Nagy A, Batai B, Balogh A, Illés S, Mikala G, Nagy N, et al. Quantitative analysis and monitoring of EZH2 mutations using liquid biopsy in follicular lymphoma. *Genes (Basel).* 2020;**11**:785.
33 Delfau-Larue MH, van der Gucht A, Dupuis J, Jais JP, Nel I, Beldi-Ferchiou A, et al. Total metabolic tumor volume, circulating tumor cells, cell-free DNA: distinct prognostic value in follicular lymphoma. *Blood Adv.* 2018;**2**:807–16.
34 Sarkozy C, Baseggio L, Feugier P, Callet-Bauchu E, Karlin L, Seymour JF, et al. Peripheral blood involvement in patients with follicular lymphoma: a rare disease manifestation associated with poor prognosis. *Br J Haematol.* 2014;**164**:659–67.
35 Zohren F, Bruns I, Pechtel S, Schroeder T, Fenk R, Czibere A, et al. Prognostic value of circulating Bcl-2/IgH levels in patients with follicular lymphoma receiving first-line immunochemotherapy. *Blood.* 2015;**126**:1407–14.
36 Scherer F, Kurtz DM, Diehn M, Alizadeh AA. High-throughput sequencing for noninvasive disease detection in hematologic malignancies. *Blood.* 2017;**130**:440–52.
37 McDonald A, Thomas E, Daigle S, Morschhauser F, Salles G, Ribrag V, et al. Updated report on identification of molecular predictors of tazemetostat response in an ongoing NHL phase 2 study. *Blood.* 2018;**132**:4097.
38 Morin RD, Johnson NA, Severson TM, Mungall AJ, An J, Goya R, et al. Somatic mutations altering EZH2 (Tyr641) in follicular and diffuse large B-cell lymphomas of germinal-center origin. *Nat Genet.* 2010;**42**:181–5.
39 Morin RD, Mendez-Lago M, Mungall AJ, Goya R, Mungall KL, Corbett RD, et al. Frequent mutation of histone-modifying genes in non-Hodgkin lymphoma. *Nature.* 2011;**476**:298–303.
40 Bodor C, O'Riain C, Wrench D, Matthews J, Iyengar S, Tayyib H, et al. EZH2 Y641 mutations in follicular lymphoma. *Leukemia.* 2011;**25**:726–9.
41 Camus V, Viennot M, Lequesne J, Viailly P-J, Elodie Bohers, Bessi L, et al. Targeted genotyping of circulating tumor DNA for classical Hodgkin lymphoma monitoring: a prospective study. *Haematologica.* 2021;**106**:154–62.
42 Spina V, Bruscaggin A, Cuccaro A, Martini M, Di Trani M, Forestieri G, et al. Circulating tumor DNA reveals genetics, clonal evolution, and residual disease in classical Hodgkin lymphoma. *Blood.* 2018;**131**:2413–25.
43 Sobesky S, Mammadova L, Cirillo M, Drees EEE, Mattlener J, Dörr H, et al. In-depth cell-free DNA sequencing reveals genomic landscape of Hodgkin's lymphoma and facilitates ultrasensitive residual disease detection. *Med (N Y).* 2021;**2**:1171–93 e11.
44 Camus V, Stamatoullas A, Mareschal S, Viailly PJ, Sarafan-Vasseur N, Bohers E, et al. Detection and prognostic value of recurrent exportin 1 mutations in tumor and cell-free circulating DNA of patients with classical Hodgkin lymphoma. *Haematologica.* 2016;**101**:1094–101.
45 Rivas-Delgado A, Nadeu F, Enjuanes A, Casanueva-Eliceiry S, Mozas P, Magnano L, et al. Mutational landscape and tumor burden assessed by cell-free DNA in diffuse large B-cell lymphoma in a population-based study. *Clin Cancer Res.* 2021;**27**:513–21.
46 Fernandez-Miranda I, Pedrosa L, Llanos M, Franco FF, Gómez S, Martín-Acosta P, et al. Monitoring of circulating tumor DNA predicts response to treatment and early progression in follicular lymphoma: results of a prospective pilot study. *Clin Cancer Res.* 2022;**29**:209–20.
47 Huet S, Xerri L, Tesson B, Mareschal S, Taix S, Mescam-Mancini L, et al. EZH2 alterations in follicular lymphoma: biological and clinical correlations. *Blood Cancer J.* 2017;**7**:e555.
48 Roschewski M, Dunleavy K, Pittaluga S, Moorhead M, Pepin F, Kong K, et al. Circulating tumour DNA and CT monitoring in patients with untreated diffuse large B-cell lymphoma: a correlative biomarker study. *Lancet Oncol.* 2015;**16**:541–9.
49 Distler A, Lakhotia R, Phelan JD, Pittaluga S, Melani C, Muppidi JR, et al. A prospective study of clonal evolution in follicular lymphoma: circulating tumor DNA correlates with overall tumor burden and fluctuates over time without therapy. *Blood.* 2021;**138**:1328.
50 Sarkozy C, Huet S, Carlton VE, Fabiani B, Delmer A, Jardin F, et al. The prognostic value of clonal heterogeneity and quantitative assessment of plasma circulating clonal IG-VDJ sequences at diagnosis in patients with follicular lymphoma. *Oncotarget.* 2017;**8**:8765–74.
51 Kurtz DM, Scherer F, Jin MC, Soo J, Craig AFM, Esfahani MS, et al. Circulating tumor DNA measurements as early outcome predictors in diffuse large B-cell lymphoma. *J Clin Oncol.* 2018;**36**:2845–53.
52 Lakhotia R, Melani C, Dunleavy K, Pittaluga S, Saba N, Lindenberg L, et al. Circulating tumor DNA predicts therapeutic outcome in mantle cell lymphoma. *Blood Adv.* 2022;**6**:2667–80.
53 Kurtz DM, Green MR, Bratman SV, Scherer F, Liu CL, Kunder CA, et al. Noninvasive monitoring of diffuse large B-cell lymphoma by immunoglobulin high-throughput sequencing. *Blood.* 2015;**125**:3679–87.
54 Lauer EM, Mutter J, Scherer F. Circulating tumor DNA in B-cell lymphoma: technical advances, clinical applications, and perspectives for translational research. *Leukemia.* 2022;**36**:2151–64.
55 Pott C, Wellnitz D, Ladetto M. Minimal residual disease in follicular lymphoma. *Ann Lymphoma.* 2021;**5**:32.

Correspondence: Csaba Bödör, Department of Pathology and Experimental Cancer Research, 26 Ulloi ut, Budapest, Hungary. Email: bodor.csaba1@semmelweis.hu

Supporting Information

Additional Supporting Information may be found in the online version of this article:

Table S1. Detailed histological, clinical and radiological information of the patients. BM: bone

marrow (percentage of infiltrating tumor cells). FLIPI: Follicular Lymphoma International Prognostic Index. GCB-DLBCL: germinal center B-cell like diffuse large B-cell lymphoma. HL: Hodgkin lymphoma. LB: liquid biopsy. LDH: lactate dehydrogenase. LG: low grade. NA: not available. PET/CT: 18F-fluorodeoxyglucose positron emission tomography combined with computer tomography. SUV max: maximized 18-fluorodeoxy glucose standardized uptake value. TB: tissue biopsy.

Table S2. Content of the two multiplex PCR mixes with unique single tube Bio-Rad© assay identifiers.

Table S3. Comparison of the analytical sensitivity of single vs multiplex PCR amplification. Dilution series were carried out on diagnostic formalin fixed paraffin embedded tissue biopsy samples. The variant allele frequencies (VAF) of the initial samples were multiplied by the level of the dilution point where the signal was last detected in triplicates for calculating the limit of detection (LOD) of each assay. For example, if the initial VAF was 20% and the signal was last detected at 1.000x (10–1) dilution point, the LOD was determined to be 0.2 x 0.1 = 0.02. Analytical sensitivity did not change considerably for mutations p.A682G and p.Y646F/C/S/N. Analytical sensitivity decreased in the multiplex PCR set up for p.A692V and p.Y646H but did not exceed one log difference and remained below 0.1%.

Table S4. EZH2 mutation status of all tissue and liquid biopsy (TB, LB) samples included in the study. VAF: variant allele frequency.

Table S5. Baseline patient characteristics and clinical data stratified by EZH2 mutation status at the time of diagnosis. Here, transformation was only considered if it occurred at the time of relapse after classical follicular lymphoma at the time of diagnosis. BM: bone marrow. GCB-DLBCL: germinal center B-cell like diffuse large B-cell lymphoma. FLIPI: Follicular Lymphoma International Prognostic Index. R-B: rituximab plus bendamustine. R-CHOP: rituximab plus cyclophosphamide,doxorubicin, vincristine and prednisone. R-CVP: rituximab plus cyclophosphamide, vincristine and prednisone.

Table S6. EZH2 mutation status of paired tissue biopsy samples (nodal/extranodal samples vs bone marrow (BM) samples). D: diagnosis. R: relapse/progression.

Table S7. Association between histological, clinical, radiological variables and EZH2 mutation status and EZH2 variant allele frequencies. BM: bone marrow. C1D1: cycle 1 day 1. C2D1:C32 cycle 2 day 1. C3D1: cycle 3 day 1. D: diagnosis. FLIPI: FLIPI: Follicular Lymphoma International Prognostic Index. GCB-DLBCL: germinal center B-cell like diffuse large B-cell lymphoma. LB: liquid biopsy. LDH: lactate dehydrogenase. LG: low grade. MT: mutant. PBMNC: peripheral blood mononuclear cell. PET/CT: 18F-fluorodeoxyglucose positron emission tomography combined with computer tomography. R: relapse. SUV max: maximized 18-fluorodeoxy glucose standardized uptake value. TB: tissue biopsy. VAF: variant allele frequency. WT:wild-type.

Table S8. Result of EZH2 monitoring on longitudinally collected samples and detailed clinical data of 23 EZH2 mutant patients. Treatment lines, under longitudinal samples were collected are marked with an asterix. ABVD: doxorubicin, bleomycin, vinblastine and dacarbazine. B: bendamustine monotherapy. C1D1: cycle 1 day 1. C2D1: cycle 2 day 1. C3D1: cycle 3 day 1. C4D1: cycle 4 day 1. C5D1: cycle 5 day 1. C6D1: cycle 6 day 1. CMR: complete metabolic remission. LB: liquid biopsy. PD: progressive disease. PR: partial remission. R2: rituximab plus lenalidomide. R-B: rituximab plus bendamustine. R-CHOP: rituximab plus cyclophosphamide, doxorubicin, vincristine and prednisone. R-CVP: rituximab plus cyclophosphamide, vincristine and prednisone. R-DHAP: rituximab plus dexamethasone, high-dose cytarabine and cisplatin. VAF: variant allele frequency. WW: watch and wait.

Table S9. Comparison of the EZH2 mutation status between paired liquid (LB) and peripheral blood mononuclear cell (PBMNC) samples. VAF: variant allele frequency.

Figure S1. A-B: Droplet digital PCR dotplots after applying the two multiplex assay mixes to a pool of samples harboring the corresponding four and three EZH2 mutations plus wild-type (WT) DNA. In this scenario, where all four and three mutation types are present, the two assay mixes generate up to 12 and 10 distinct fluorescent clusters, respectively. Fluorescent clusters harboring only one of the mutant DNA fragments are colored blue, droplets harboring WT DNA are colored green, clusters harboring both mutant and WT are colored orange, droplets without template DNA are grey.

Mutant droplet clusters were always compared to positive controls harboring a known EZH2 mutation tested in the same run. To determine the variant allele frequency of a mutation we selectively outlined the droplets containing the mutation with the "lasso" function of the QuantaSoft software, then similarly we outlined the corresponding WT droplets (WT for exon 16 and WT for exon 16 + 18, if the mutation is p.Y646X and WT for exon 18 and WT for exon 16 + 18, if the mutation is p.A682G or p.A692V). To determine the detected copy number if no mutation was present, we outlined only droplets WT for exon 16 and WT simultaneously for exon 16 and 18.**Figure S2. A-B**: Comparison between statistical sensitivity, specificity and negative predictive value (NPV) of liquid biopsy (LB) and tissue biopsy (TB) based EZH2 mutation detection analysis of the 114 follicular lymphoma patients with paired TB and LB samples. We determined the specificity and the NPV of the TB and the LB based EZH2 mutation detection compared to the LB or to the TB based approach, respectively. We did not consider those samples false positive where the EZH2 mutation was only found in the LB sample, therefore statistical sensitivity was calculated from the sum of mutant samples in TB and LB. MT: mutant. WT: wild-type.

Figure S3. A: Linear regression analysis of paired tissue (TB) and pre-treatment liquid biopsy (LB) EZH2 VAF values. B-E: Connection between LB EZH2 variant allele frequency (VAF) and clinical parameters. Parenchymal organ or skin involvements were considered as extranodal involvement, bone marrow infiltration was evaluated separately. LDH: lactate dehydrogenase.

Figure S4. Illustration of clonal expansion of the EZH2 mutant clone in the case of Pt-118. The patient was treated with upfront rituximab monotherapy and subsequently reached complete remission. Liquid biopsy (LB) sample collected at this timepoint was found to be EZH2 wild-type. Ten months later the patient relapsed to an EZH2 mutant FL, at this timepoint the EZH2 mutation could be detected in the peripheral blood with a relatively high variant allele frequency (VAF). When analyzed retrospectively, the same mutation could be detected in the LB specimen seven months prior to relapse with low VAF.

Figure S5. Comparison of EZH2 variant allele frequencies (VAF) between liquid biopsy (LB) and peripheral blood mononuclear cell samples (PBMNC). VAFs are displayed on a log2 scale. Original VAFs (LB VAF range: 0.1–74.0%, PBMNC VAF range: 0.008–0.77%) were multiplied by 1000 (to avoid negative and zero values), then transformed to a log2 scale. Values are sorted from left to right in a descending order based on LB VAFs. Cases with detectable EZH2 mutations in the PBMNC sample are clustered to the left. ■